A FERROFLUID LUBRICATION OF A ROUGH, POROUS INCLINED SLIDER BEARING WITH SLIP VELOCITY

Nitin D Patel[1], Gunamani Deheri[2]

[1],[2]Department of Mathematics, Sardar Patel University,
Vallabh Vidhyanagar-388120, India

Email: [1]ndpatel2002@gmail.com

ABSTRACT

An endeavor has been made to investigate the performance of a ferrofluid lubricated rough porous inclined slider bearing considering slip velocity. Jenkins model for the flow of magnetic fluid has been adopted. It is observed that although magnetization introduces a positive effect on the performance, the bearing suffers owing to transverse surface roughness. The performance of the bearing system can be made to improve by suitably choosing the magnetization parameter and slip coefficient in the case of negatively skewed roughness, which becomes more sharp with the occurrence of variance (-ve).

KEYWORDS: Porosity, Roughness, Pressure, Load, Friction, Jenkins Model.

1.0   INTRODUCTION

While, Jenkins (1971) used a simple continuum model for a paramagnetic fluid to analyze a simple shearing flow and parallel flow through a pipe and examined the possibility of maintaining a steady circular flow in a circular cylinder by rotating a magnetic field, Verma and Singh (1981) considered the interaction between magnetic and mechanical forces in the case of flow of an incompressible paramagnetic fluid through a porous annulus subjected to the external magnetic field. Shah and Bhat (2003) studied the behavior of a porous exponential slider bearing with a ferrofluid lubricant whose flow was governed by Jenkins model taking velocity slip into account. It was observed that the load carrying capacity as well as the friction decreased when the slip parameter increased. However, increase in the material parameter caused decreased load carrying capacity and increased friction. The position of centre of pressure was not affected significantly by the slip parameter but the position of centre of pressure shifted towards the bearing inlet for large values of material parameter. Performance of a slider bearing

with its stator having circular convex pad surface was subjected to investigation by Shah and Bhat (2004) under the presence of ferrofluid lubrication when Jenkins model described the flow. It was found that the load carrying capacity increased with the increasing values of field or the film thickness ratio and decreasing value of the material parameter. The friction force on the slider decreased with increasing film thickness ratio while the position of centre of pressure shifted towards the outlet. Chaves *et.al.* (2006) obtained direct measurements of the bulk flow of a ferrofluid in a uniform rotating magnetic field using the ultrasonic velocity profile method. Zakaria *et.al.* (2011) explored the static and dynamic performance characteristics of finite journal bearing lubricated with a non Newtonian ferrofluid in the presence of an external magnetic field using the spectral method technique. Here it was shown that the magnetic parameter played an important role in administrating the stability behavior.

Slider bearings mainly, are designed for supporting the transverse load in engineering system. The performance characteristics of a bearing system have been analyzed taking various film shapes into consideration (Cameron (1966), Agrawal (1986), Ajwalia (1984), and Andharia *et.al.* (1998)). In order to improve upon the bearing performance many investigations made use of the couple stress fluid model regarding the fluid film lubrication. The fact that use of couple stress fluid increased the load carrying capacity and extended the response time of squeeze film action was established in the studies by (Ramanaiah (1979a, 1979b), Lin (1997a, 1997b, 1997c, 2001) and Mokhiamer (1999)). Lin (2004) analyzed the couple stress effect on the steady state performance of a wide parabolic shaped slider bearing and found that the couple stress effect resulted in an improvement in the steady state performance.

Fluids with strong magnetic properties have drawn considerable attentions in recent years. For lubricating the bearing system in technical applications in the domain of nano scale science and technology significant progress has been made. Therefore, the use of magnetic fluid lubrication adds an additional importance from nano science point of view. Magnetic fluid consists of colloidal magnetic nano particles dispersed with the aid of surfactants in a continuous career phase. In fact, Magnetic fluid is a typical hybrid of soft material and the nano particles. The average diameter of the dispersed particles ranges from 5 to 10 nm. The ferrofluids contain enormous magnetic nano particles and therefore can be influenced by either parallel or perpendicular magnetic field. Agrawal [8] analyzed the performance of a ferrofluid lubricated plane inclined slider bearing and proved that the performance was relatively better than the corresponding bearing

system with a conventional lubricant. The discussion of Bhat and Patel (1991) regarding the exponential slider bearing with a ferrofluid lubricant suggested that the magnetic fluid lubricant caused increased load carrying capacity while the friction remained almost unchanged. The study of Bhat and Deheri (1991a) revealed that the magnetic fluid sharply increased the load carrying capacity for a squeeze film performance between porous annular disks. The contribution of Bhat and Deheri (1991b) confirmed the positive impact of magnetic fluid lubrication on the steady state performance of a porous composite slider bearing.

It is well known that the roughness of the bearing surfaces retards the motion of the lubricant thereby affecting adversely the bearing system. Tzeng and Saibel (1967) recognized the random character of the roughness and adopted a stochastic approach to study the effect of surface roughness. This modeling of Tzeng and Saibel (1967) was modified by Christensen and Tonder (1969a, 1969b and 1970) to deal with the effect of surface roughness in general, on the performance of the bearing system. Below are some of the investigations which made use of the method of Christensen and Tonder (1969a, 1969b and 1970) to account for surface roughness. The magnetic fluid lubrication of a transversely rough slider bearing was investigated by Deheri *et.al*. (2005) by taking various film shapes in to consideration. The effect of transverse surface roughness was adverse in general while magnetic fluid lubricant increased the load carrying capacity. This squeeze film performance in the case of longitudinal surface roughness was observed to be relatively better than the corresponding one with transverse surface roughness as established by Deheri *et.al*. (2004).The hydrodynamic lubrication of rough slider bearings was studied by Nanduvinamani *et.al*. (2003) taking couple stress effect in to account. Recently, Patel and Deheri (2011) analyzed the ferrofluid lubrication of a plane inclined slider bearing with velocity slip. The flow of the ferrofluid was based on Shliomis model. Here, it was shown that the magnetization could reduce the adverse effect of surface roughness up to some extent when suitable values of slip parameter were in place.

Here, it has been sought to study the hydrodynamic lubrication of a rough, porous, plane inclined slider bearing with slip velocity.

2.0   ANALYSIS

The geometry and configuration of the ferrofluid lubricant based plane inclined slider bearing is presented below in Figure 1.
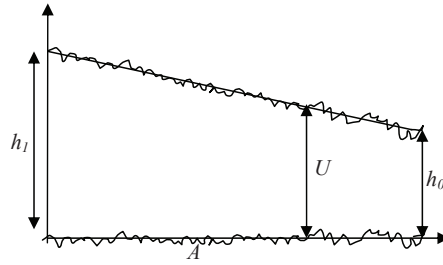
Figure 1 Configuration of the Bearing System

Following Bhat (2003),

The film thickness is taken as

$$\bar{h} = a - (a-1)X, \quad a = \frac{h_1}{h_0}, \ \bar{h} = \frac{h}{h_0}, X = \frac{x}{A}$$

Thus, incorporating the effects of porosity and slip, the associated Reynolds type equation turns out to be

$$\frac{d}{dx}\left[\frac{g(h)}{1 - \frac{\rho\alpha^2 \bar{\mu}H}{2\eta}} \frac{d}{dx}\left(p - \frac{\mu_0 \bar{\mu}}{2} H^2 \right) \right] = 6\eta U \frac{dh}{dx} + 12\eta \dot{h}_0$$

(1)

where

$$g(h) = \left\{ h^3 + 3\alpha h^2 + 3\left(\alpha^2 + \sigma^2 \right)h + 3\sigma^2 \alpha + \alpha^3 + \varepsilon + 12\phi h \right\} \frac{(4+sh)}{(2+sh)}$$

(2)

Taking $H^2 = KA^2 \sin(\pi X)$ and introducing the dimensionless quantities

$$X = \frac{x}{A}, \bar{h} = \frac{h}{h_0}, \mu^* = \frac{K\mu_0 \bar{\mu} h_0^2 A}{\eta U}, \bar{\alpha}^2 = \frac{\rho\alpha^2 \bar{\mu}A\sqrt{K}}{2\eta}, P = \frac{h_0^3 p}{\eta A^2 \dot{h}_0}, \beta_1 = \frac{h_0^3}{2\dot{h}_0 A}$$

$$W = \frac{h_0^3 w}{\eta A^4 \dot{h}_0}, \ F = \frac{-h_0 f}{\eta L^2 \dot{h}_0}, \ Y = \frac{\bar{X}}{A}, \ \bar{\alpha} = \frac{\alpha}{h_0}, \bar{\sigma} = \frac{\sigma}{h_0}, \bar{\varepsilon} = \frac{\varepsilon}{h_0^3}, \ \bar{s} = sh_0, \ \bar{\psi} = \frac{\phi h}{h_0^3}$$

Equation (1) yields on integration,

$$\frac{d}{dx}\left[P - \frac{1}{2}\mu^{*}X(1-X)\right] = \frac{6}{g(\bar{h})}\left(A_1 \frac{(2+\bar{s}\,\bar{h})}{(1+\bar{s}\,\bar{h})}\bar{h} - \beta^{-1}X + A_2\,Q\right)\left(1 - \bar{\alpha}'^{2}\sqrt{X(1-X)}\right)$$

(3)

where

$$A_1 = 3\left(\bar{\alpha}^2 + \bar{\sigma}^2\right)$$

$$A_2 = \left(3\bar{\sigma}^2\bar{\alpha} + \bar{\alpha}^3 + \bar{\varepsilon} + 12\bar{\psi}\right)$$

and

$$g(\bar{h}) = \left\{\bar{h}^3 + 3\bar{\alpha}\bar{h}^2 + A_1 + A_2\right\}\frac{(4+\bar{s}\,\bar{h})}{(2+\bar{s}\,\bar{h})}$$

(4)

Solving Equation (3) under the boundary conditions

$$P\,(1) = P\,(a) = 0$$

yields

$$P = \frac{1}{2}\mu^{*}\sin(\pi X) + \left\{6\int_{0}^{1}\frac{1}{g(\bar{h})}\left(A_1\frac{(2+\bar{s}\,\bar{h})}{(1+\bar{s}\,\bar{h})}\bar{h} - \beta^{-1}X + A_2 Q\right)\right\}\left(1 - \bar{\alpha}'^{2}\sqrt{X(1-X)}\right)dX$$

(5)

where

$$Q = -\int_{0}^{1}\frac{\dfrac{1}{g(\bar{h})}\left(A_1\dfrac{(2+\bar{s}\,\bar{h})}{(1+\bar{s}\,\bar{h})}\bar{h} - \beta^{-1}X\right)\left(1 - \bar{\alpha}'^{2}\sqrt{X(1-X)}\right)dX}{\dfrac{1}{g(\bar{h})}\left(1 - \bar{\alpha}'^{2}\sqrt{X(1-X)}\right)dX}$$

(6)

The load capacity *W*, frictional force *F* and Position of centre of pressure *Y* are respectively expressed in dimensionless form as

$$W = \frac{2\mu^{*}}{\pi} - \left\{6\int_{0}^{1}\frac{X}{g(\bar{h})}\left(A_1\frac{(2+\bar{s}\,\bar{h})}{(1+\bar{s}\,\bar{h})}\bar{h} - \beta^{-1}X + A_2 Q\right)\right\}\left(1 - \bar{\alpha}'^{2}\sqrt{X(1-X)}\right)dX$$

(7)

$$F = -\int_0^1 \left[\frac{1}{A_1 \frac{(2+\bar{s}\,\bar{h})}{(1+\bar{s}\,\bar{h})}\bar{h}} + \frac{1}{\alpha\bar{h}^2}\left(A_1 \frac{(2+\bar{s}\,\bar{h})}{(1+\bar{s}\,\bar{h})}\bar{h} - \beta^{-1}X + A_2 Q \right) \right] dX$$

(8)

and

$$Y = \frac{1}{W}\left[\frac{\mu^*}{\pi} - \left\{ 3\int_0^1 \frac{X^2}{g(\bar{h})}\left(A_1 \frac{(2+\bar{s}\,\bar{h})}{(1+\bar{s}\,\bar{h})}\bar{h} - \beta^{-1}X + A_2 Q \right)\left(1 - \bar{\alpha}'^2\sqrt{X(1-X)}\right)dX \right\} \right]$$

(9)

3.0   RESULTS AND DISCUSSION

It is noticed that dimensionless pressure distribution is governed by the Equation [5] while the distribution of load carrying capacity in non-dimensional form is determined by [7]. In addition the friction is calculated from Equation [8] and the non dimensional position of centre of pressure is governed by the Equation [9]. Further, taking the roughness parameter to be zero this investigation reduces to the performance of a plane inclined slider bearing having smooth surfaces with slip velocity under the presence of a magnetic fluid lubricant. Besides, setting μ* to be zero this study becomes the study of the performance of a plane inclined slider bearing with slip velocity which in turn reduces to the study of Basu *et.al.* (2005) in the absence of slip velocity. From Equations [5] and [7] it is observed that the dimensionless pressure increases by

$$\frac{1}{2}\mu^* \sin(\pi X)$$

while the non-dimensional load carrying capacity gets enhanced by

as compared to the case of conventional lubricant.

The variation of load carrying capacity with respect to magnetization parameter displayed in Figures 2-8 indicates that the magnetization increases the load carrying capacity significantly. This effect is relatively less in the case of material parameter.
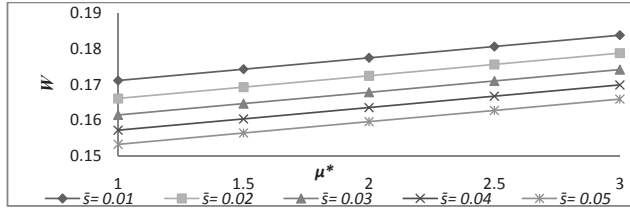
Figure 2 Variation of load carrying capacity with respect to μ^* and $\bar{s}$
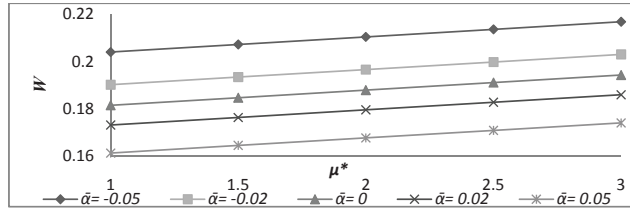
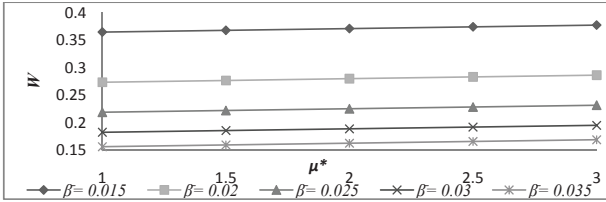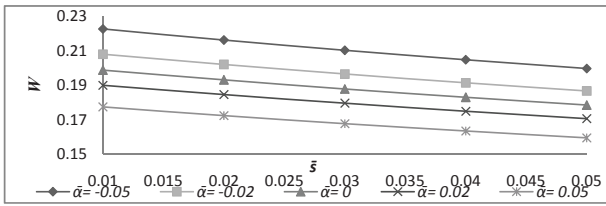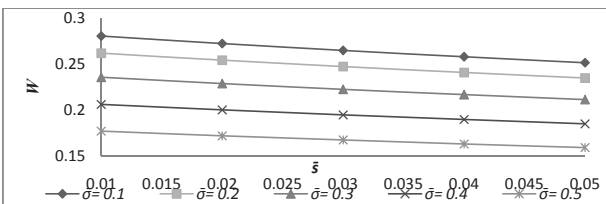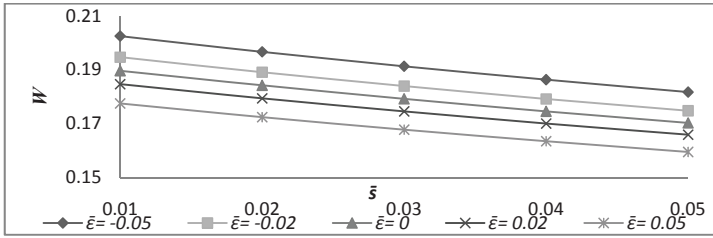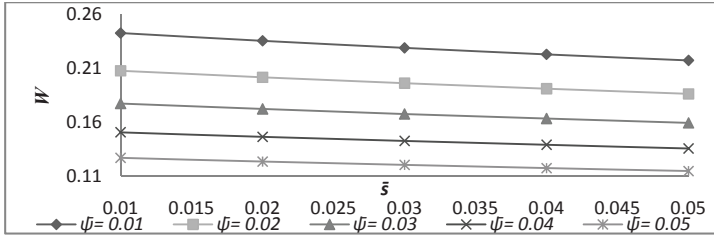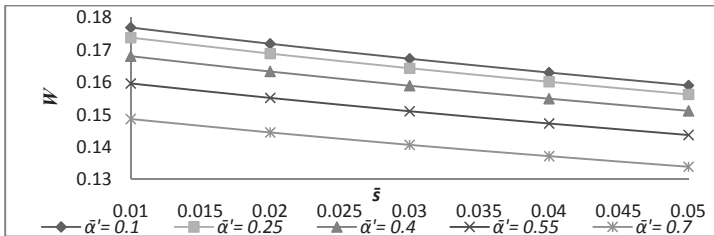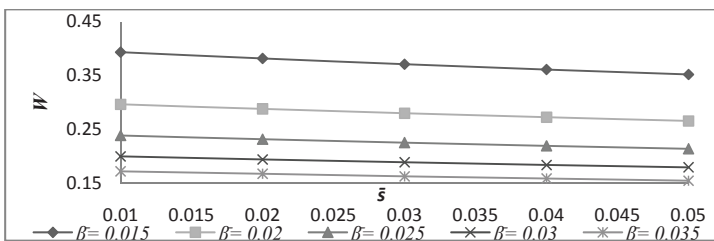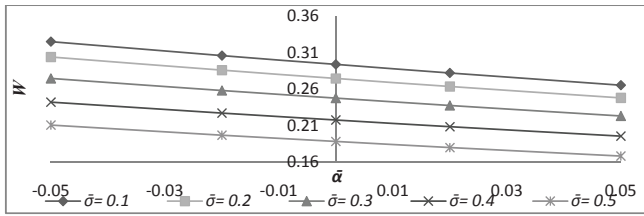Figure 3 Variation of load carrying capacity with respect to μ^* and $\bar{\alpha}$
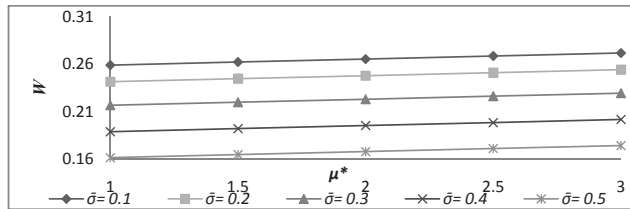
Figure 4 Variation of load carrying capacity with respect to μ^* and $\bar{\sigma}$
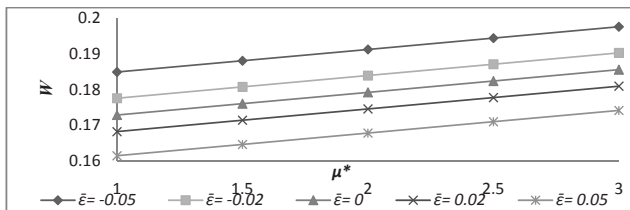
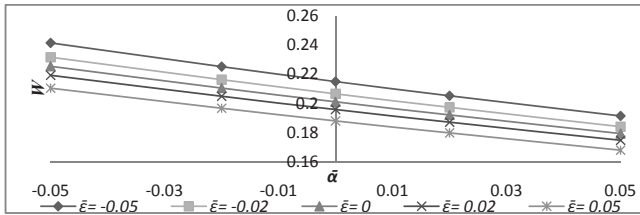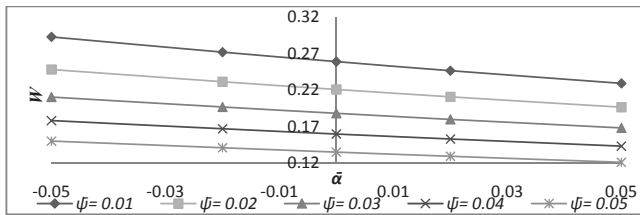Figure 5 Variation of load carrying capacity with respect to μ^* and $\bar{\varepsilon}$
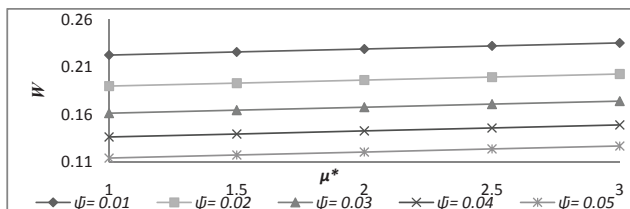
Figure 6 Variation of load carrying capacity with respect to μ^* and $\bar{\psi}$
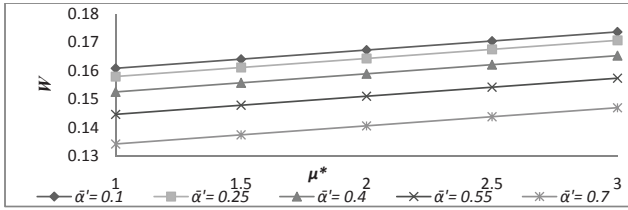
Figure 7 Variation of load carrying capacity with respect to μ^* and $\bar{\alpha}'$

Figure 8 Variation of load carrying capacity with respect to μ^* and $\bar{\beta}$

The variation of load carrying capacity with respect to the slip parameter is presented in Figures 9-14. It is clear that the load carrying capacity decreases considerably with increasing values of slip parameter.
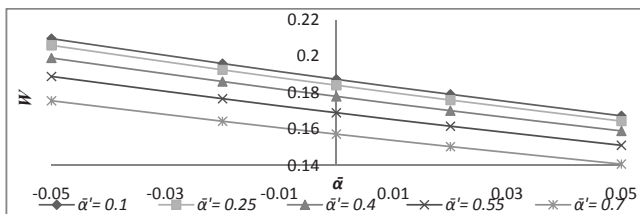

Figure 9 Variation of load carrying capacity with respect to $\bar{s}$ and $\bar{\alpha}$

Figure 10 Variation of load carrying capacity with respect to $\bar{s}$ and $\bar{\sigma}$

Figure 11 Variation of load carrying capacity with respect to $\bar{s}$ and $\bar{\varepsilon}$

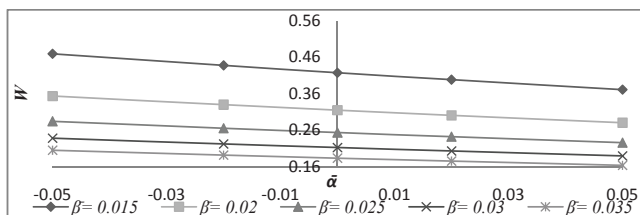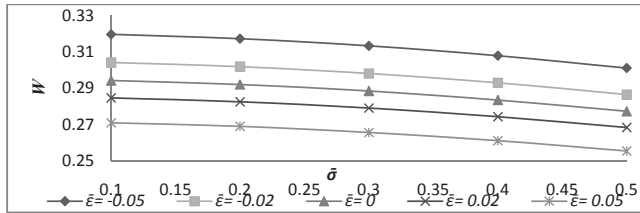Figure 12 Variation of load carrying capacity with respect to $\bar{s}$ and $\bar{\psi}$

Figure 13 Variation of load carrying capacity with respect to $\bar{s}$ and $\overline{\alpha}'$

Figure 14 Variation of load carrying capacity with respect to $\bar{s}$ and $\overline{\beta}$

The effect of the variance on the distribution of load carrying capacity is presented in Figures 15-19. It is clearly seen that the variance (+ve) decreases the load carrying capacity while the variance (-ve) increases the load carrying capacity.
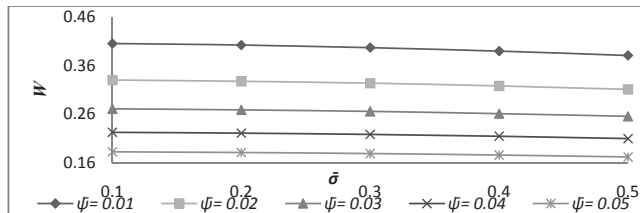
Figure 15 Variation of load carrying capacity with respect to $\bar{\alpha}$ and $\bar{\sigma}$.

Figure 16 Variation of load carrying capacity with respect to $\bar{\alpha}$ and $\bar{\varepsilon}$

Figure 17 Variation of load carrying capacity with respect to $\bar{\alpha}$ and $\bar{\psi}$
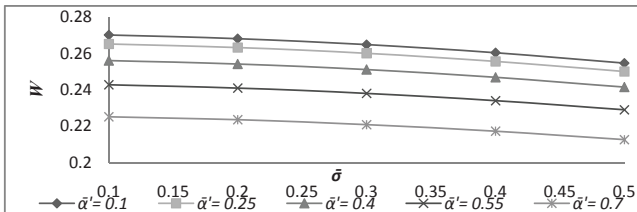

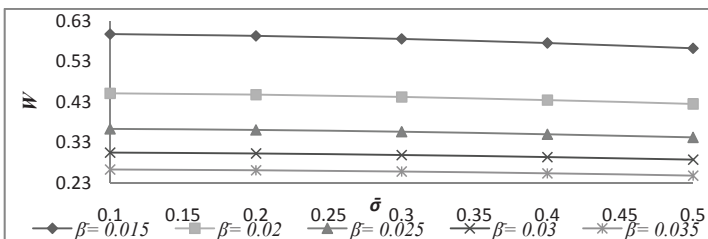Figure 18 Variation of load carrying capacity with respect to $\bar{\alpha}$ and $\overline{\alpha}'$

Figure 19 Variation of load carrying capacity with respect to $\bar{\alpha}$ and $\overline{\beta}$

The effect of standard deviation depicted in Figures 20-23 suggests that the standard deviation has a considerable adverse effect on the performance of the bearing system in the sense that it decreases the load carrying capacity considerable. The effect of higher values of porosity on load carrying capacity is negligible with respect to the standard deviation, as can be noticed.

Figure 20 Variation of load carrying capacity with respect to $\bar{\sigma}$ and $\bar{\varepsilon}$

Figure 21 Variation of load carrying capacity with respect to $\bar{\sigma}$ and $\bar{\psi}$

Figure 22 Variation of load carrying capacity with respect to $\bar{\sigma}$ and $\overline{\alpha}'$

Figure 23 Variation of load carrying capacity with respect to $\bar{\sigma}$ and $\overline{\beta}$

Figures 24-26 representing the effect of skewness suggest that the skewness follows the path of the variance regarding the trends of load carrying capacity.
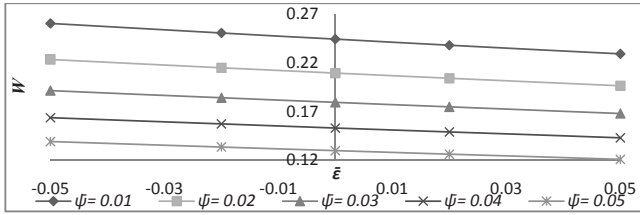

Figure 24 Variation of load carrying capacity with respect to $\bar{\varepsilon}$ and $\bar{\psi}$
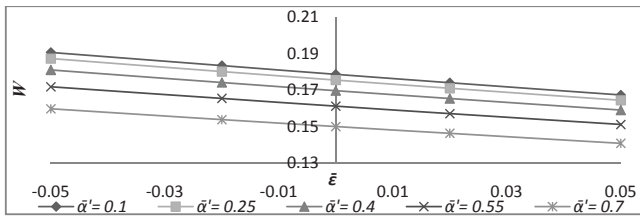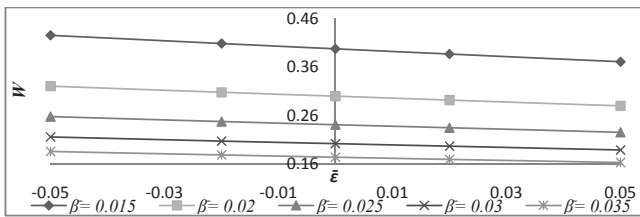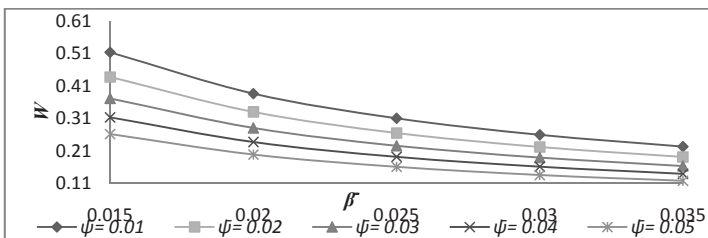

Figure 25 Variation of load carrying capacity with respect to $\bar{\varepsilon}$ and $\overline{\alpha}'$

Figure 26 Variation of load carrying capacity with respect to $\bar{\varepsilon}$ and $\overline{\beta}$

The fact that material parameter decrease the load carrying capacity significantly can be found from Figures 28-29.

Figure 27 Variation of load carrying capacity with respect to $\overline{\beta}$ and $\bar{\psi}$
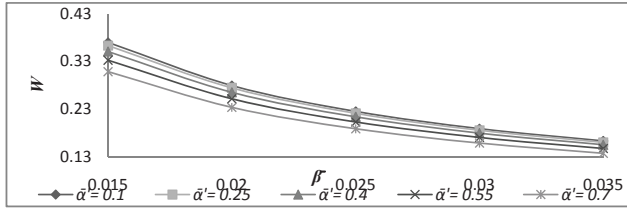
Figure 28 Variation of load carrying capacity with respect to $\bar{\beta}$ and $\vec{\alpha}$

The effect of slip parameter on the friction depicted in Figures 29-33 makes it clear that the friction reduces negligibly due to the slip parameter.
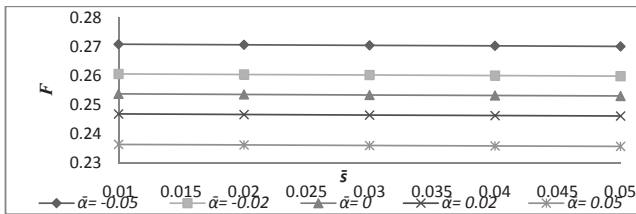

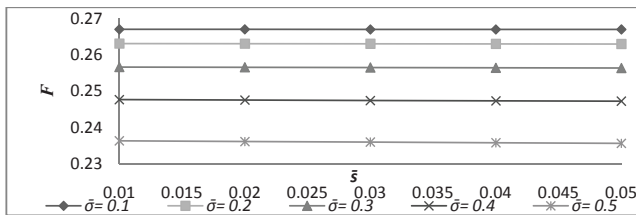Figure 29 Variation of friction with respect to $\bar{s}$ and $\bar{\alpha}$

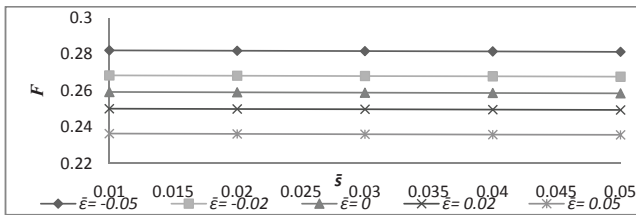Figure 30 Variation of friction with respect to $\bar{s}$ and $\bar{\sigma}$

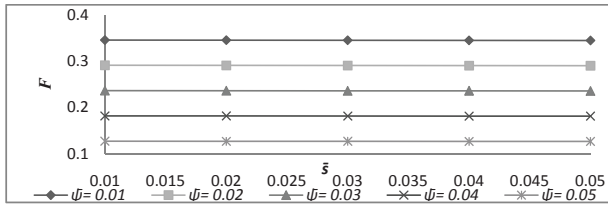Figure 31 Variation of friction with respect to $\bar{s}$ and $\bar{\varepsilon}$

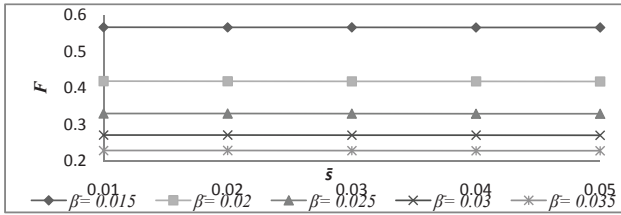Figure 32 Variation of friction with respect to $\bar{s}$ and $\bar{\psi}$

Figure 33 Variation of friction with respect to $\bar{s}$ and $\overline{\beta}$

The effect of the variance on the friction is presented in Figures 34-37. It is clearly seen that the variance (+ve) decreases the friction while the variance (-ve) increases the friction.
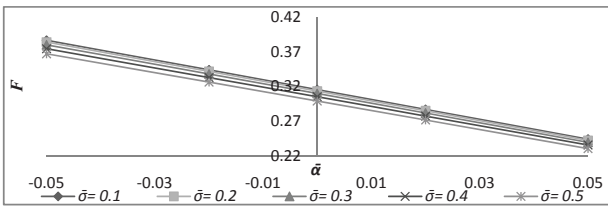

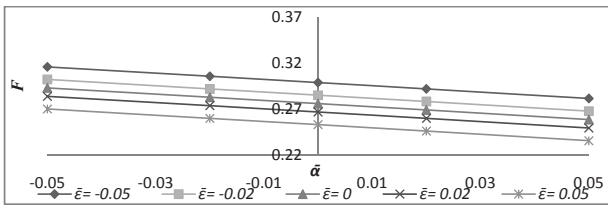Figure 34 Variation of friction with respect to $\bar{\alpha}$ and $\bar{\sigma}$

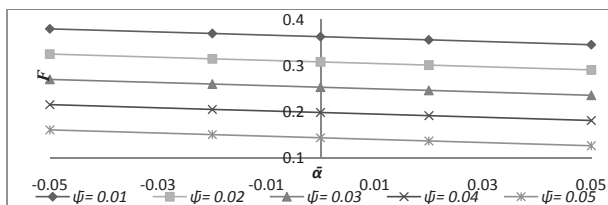Figure 35 Variation of friction with respect to $\bar{\alpha}$ and $\bar{\varepsilon}$

Figure 36 Variation of friction with respect to $\bar{\alpha}$ and $\bar{\psi}$
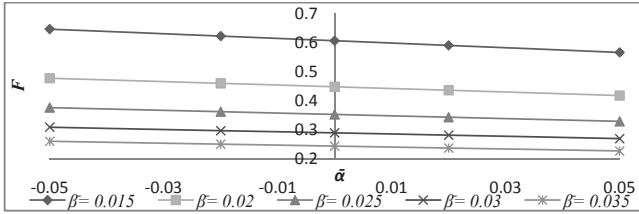
Figure 37 Variation of friction with respect to $\bar{\alpha}$ and $\bar{\beta}$

Figures 38-40 suggest that the friction reduces due to the standard deviation and this decrease in friction is more in case of skewness.

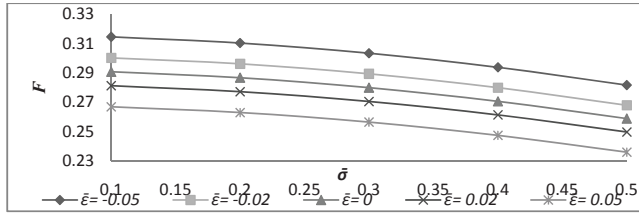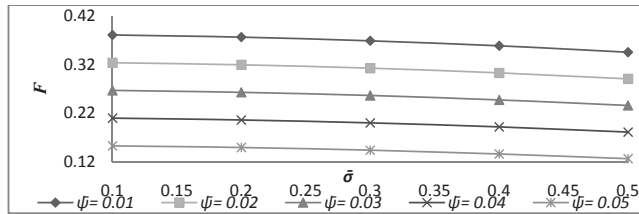Figure 38 Variation of friction with respect to $\bar{\sigma}$ and $\bar{\varepsilon}$

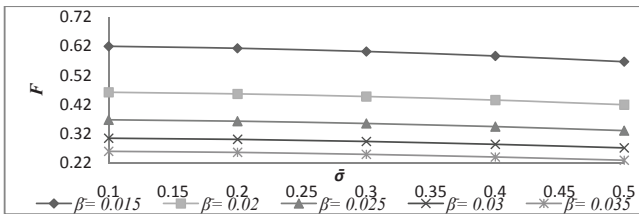Figure 39 Variation of friction with respect to $\bar{\sigma}$ and $\bar{\psi}$

Figure 40 Variation of friction with respect to $\bar{\sigma}$ and $\bar{\beta}$

The effect of skewness presented in Figures 41-42. It is clear that the skewness follows the path of the variance regarding the trends of friction.
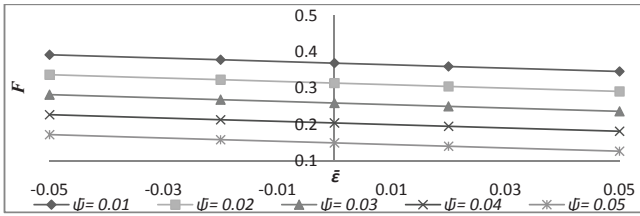
Figure 41 Variation of friction with respect to $\bar{\varepsilon}$ and $\bar{\psi}$
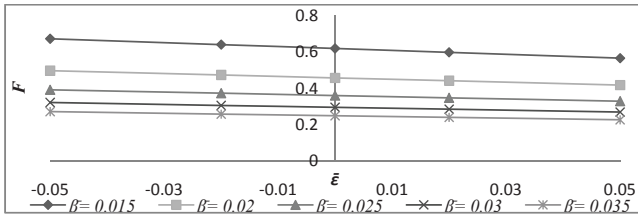
Figure 42 Variation of friction with respect to $,\bar{\varepsilon}$ and $\bar{\beta}$

The fact that material parameter decreases the friction can be seen from Figure 43.

Figure 43 Variation of friction with respect to $\bar{\beta}$ and $\bar{\psi}$

Mostly, the centre of pressure shifts towards the outlet edge as can be observed from Figures 44-48.
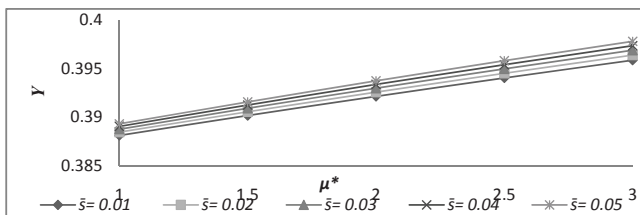
Figure 44 Variation of position of centre of pressure with respect to μ^* and $\bar{s}$
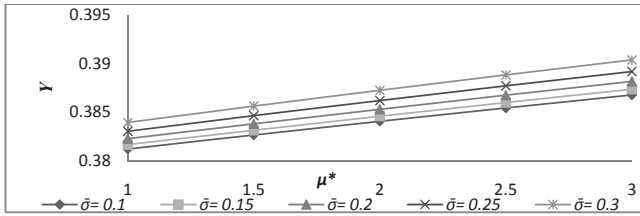
Figure 45 Variation of position of centre of pressure with respect to
μ^* and $\bar{\sigma}$
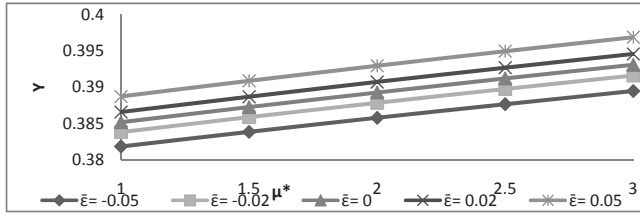
Figure 46 Variation of position of centre of pressure with respect to
μ^* and $\bar{\varepsilon}$
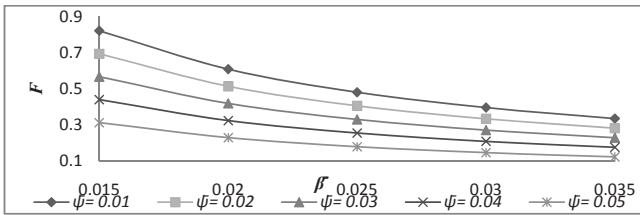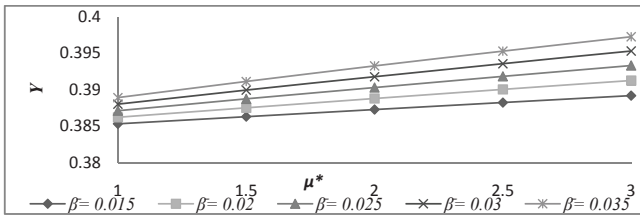

Figure 47 Variation of position of centre of pressure with respect to
μ^* and $\bar{\beta}$
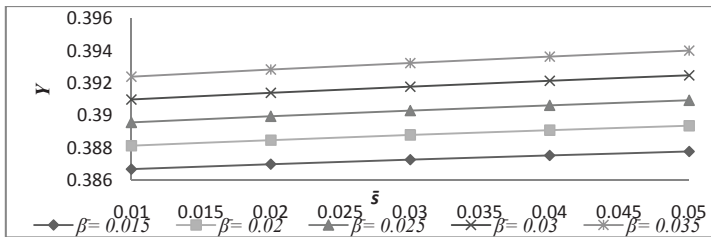

Figure 48 Variation of position of centre of pressure with respect to
$\bar{s}$ and $\bar{\beta}$

Some of the Figures presented here suggest that the decreased load carrying capacity due to the slip velocity gets further decreased due to porosity and standard deviation. Hence, this study reveals that the combined effect of porosity, standard deviation and slip parameter is

considerably adverse. However, this adverse effect can be minimized up to certain extent by the positive effect of magnetic fluid lubricant in the case of negatively skewed roughness. The variance (-ve) further hastens this process. In this compensation of the adverse effect even the material parameter plays a seminal role.

4.0 CONCLUSION

This study establishes that from the bearings life period point of view the surface roughness must be accounted for while designing the bearing system even if a suitable value of magnetization parameter has been chosen. For obtaining a relatively better performance slip has to be kept at minimum level although, material parameter has been suitably chosen.

REFERENCES

[1]   J. T. Jenkins. 1971. Some simple flows of a paramagnetic fluid. Le Journal De Physique. 32. 931.

[2]   P. D. S. Verma, M. Singh. 1981. Magnetic fluid flow through porous annulus. International Journal of Non-Linear Mechanics. 16. pp. 371-378.

[3]   R. C. Shah, M. V. Bhat. 2003. Analysis of porous exponential slider bearing lubricated with a ferrofluid considering slip velocity. Journal of the Braz. Soc. of Mech. Sci. & Eng. 3. 265.

[4]   R. C. Shah, M. V. Bhat. Ferrofluid lubrication of a slider bearing with circular convex pad. Journal of the National Science Foundation. 32. pp. 139-148.

[5]   A.S. Chaves, F. V. C. Rinaldi, S. Elborai, X. W. He, M. Zahn. 2006. Bulk flow in ferrofluids in a uniform rotating magnetic field. Physics Rev. Letter. 96. 4.

[6]   Kadry Zakaria, Magdy A. Sirwah, M. Fakharany. 2011. Theoretical study of static and dynamic characteristics for eccentric cylinders lubricated with ferrofluid. Journal of Tribology. 133. 18.

[7]   A. Cameron. 1966. The Principles of Lubrication, Longmans Green and Co. Ltd., London.

[8]   V. K. Agrawal. 1986. Magnetic fluid based porous inclined slider bearing. Wear. 107. pp. 133-139.

[9]   M. Ajwalia. 1984. Hydrodynamics lubrication of a secant shaped porous slider bearing. Ph.D thesis submitted to S. P. University, India.

[10]   P. I. Andharia, J. L. Gupta, G. M. Deheri. 1998. Effect of longitudinal surface roughness on hydrodynamic lubrication of hyperbolic slider bearings. PROC. NAT. ACAD. SCI., India, 68(A), III.

[11]   G. Ramanaiah. 1979a. Squeeze Films between Finite Plates Lubricated by Fluids with Couple Stress. Wear. Vol.54. pp. 315-320.

[12]   G. Ramanaiah. 1979b. Slider Bearings Lubricated by Fluids with Couple Stress. Wear. Vol. 52. pp. 27-36.

[13]   J. R. Lin. 1997a. Squeeze Film Characteristics of Long Partial Journal Bearings Lubricated with Couple Stress Fluids. Tribol. Int. Vol. 30. pp. 53-58.

[14]   J. R. Lin. 1997b. Effects of Couple Stresses on the Lubrication of Finite Journal Bearing. Wear. Vol. 206. pp. 171-178.

[15]   J. R. Lin. 1997c. Static Characteristics of Rotor Bearing System Lubricated with Couple Stress Fluids. Computers & Structures. Vol. 62. No. 1. pp. 175-184.

[16]   J. R. Lin. 2001. Linear Stability Analysis of Rotor Bearing System: Couple Stress Fluid Model. Computers & Structures. Vol. 79. pp. 801-809.

[17]   U. Mokhiamer, W. Crosby, H. El-Gamal. 1999. A Study of a Journal Bearing Lubricated by Fluids with Couple Stress Considering the Elasticity of the Linear. Wear. Vol. 224. pp. 191-201.

[18]   J. R. Lin, Y. M. Lu. 2004. Steady state performance of wide parabolic shaped slider bearings with a couple stresses fluid. Journal of Marine Science and Technology. Vol. 12. No.4. pp. 239-246.

[19]   M. V. Bhat, R. M. Patel. 1991. Analysis of an exponential porous slider bearing lubricated with magnetic fluid. Journal of Eng. and Tech. S.P. University. 6. pp. 19-21.

[20]   M. V. Bhat, G. M. Deheri. 1991a. Squeeze film behavior in porous annular discs lubricated with   magnetic fluid. Wear. 151. pp.123-128.

[21]   M. V. Bhat, G. M. Deheri. 1991b. Porous composite slider bearing lubricated with magnetic fluid. Japanese Journal of Applied Physics. 30. pp. 2513-2514.

[22]   S. T. Tzeng, E. A. Saibel. 1967. Surface roughness effect on slider bearing lubrication", Trans. ASME, J. Lubrication Technology. 10. pp. 334-338.

[23]   H. Christensen, K.C. Tonder. 1969a. Tribology of rough surfaces: Stochastic models of hydrodynamic lubrication. SINTEF Report No. 10/69-18.

[24]   H. Christensen, K.C. Tonder. 1969b.Tribology of rough   surfaces:

parametric study and comparison of lubrication. SINTEF Report No. 22/69-18.

[25]   H. Christensen, K. C. Tonder. 1970. The Hydrodynamic lubrication of rough bearing surfaces of finite width. ASME-ASLE lubrication conference. Paper No. 70. Lub.-7.

[26]   G. M. Deheri, P. I. Andharia, R. M. Patel. 2005. Transversely rough slider bearings with squeeze film formed by a magnetic fluid. International Journal of Applied Mechanics and Engineering. Vol. 10. No. 1. pp. 53-76.

[27]   G. M. Deheri, P. I. Andharia, R. M. Patel. 2004. Longitudinally rough slider bearings with Squeeze film formed by a magnetic fluid. Industrial Lubrication and Tribology. Vol. 56. No. 3. pp. 177-187.

[28]   N. B. Naduvinamani, Syeda Tasneem Fathima, P. S. Hiremath. 2003. Hydrodynamic lubrication rough Slider bearings with couple stress fluids. Tribology International. Vol. 36, 12. pp. 949-959.

[29]   N. D. Patel, G. M. Deheri. 2011. Shliomis model based ferrofluid lubrication of a plane inclined slider bearing with slip velocity. International Journal of fluids engineering. Vol. 3, No 3. pp. 311-324.

[30]   M. V. Bhat. 2003. Lubrication with a magnetic fluid. Team Spirit (India) Pvt. Ltd.

[31]   S. K. Basu, S. N. Sengupta, B. B. Ahuja. 2005. Fundamentals of Tribology, Prentice-Hall of Indian Private Limited, New Delhi.